

PYROMETRIC METHOD OF TEMPERATURE MEASUREMENT WITH COMPENSATION FOR SOLAR RADIATION

Henryk Madura, Mariusz Kastek, Tomasz Sosnowski, Tomasz Orzanowski

Military University of Technology, Institute of Optoelectronics, S. Kaliskiego 2, 00–908 Warsaw, Poland (✉ hmadura@wat.edu.pl, +48 22 683 9383, mkastek@wat.edu.pl, tsosnowski@wat.edu.pl, torzanowski@wat.edu.pl)

Abstract

Outdoor remote temperature measurements in the infrared range can be very inaccurate because of the influence of solar radiation reflected from a measured object. In case of strong directional reflection towards a measuring device, the error rate can easily reach hundreds per cent as the reflected signal adds to the thermal emission of an object. As a result, the measured temperature is much higher than the real one. Error rate depends mainly on the emissivity of an object and intensity of solar radiation. The position of the measuring device with reference to an object and the Sun is also important. The method of compensation of such undesirable influence of solar radiation will be presented. It is based on simultaneous measurements in two different spectral bands, short-wavelength and long-wavelength ones. The temperature of an object is derived from long-wavelength data only, whereas the short-wavelength band, the corrective one, is used to estimate the solar radiation level. Both bands were selected to achieve proportional changes of the output signal due to solar radiation. Knowing the relation between emissivity and solar radiation levels in both spectral bands, it is possible to reduce the measurement error several times.

Keywords: intensity of solar radiation, emissivity, pyrometry, radiometric temperature measurements.

© 2010 Polish Academy of Sciences. All rights reserved

1. Introduction

Results of remote temperature measurements of low-emissivity objects can be very inaccurate when the objects are under strong isolation. Especially, such a measuring situation should be avoided when solar radiation reflects directionally from a surface the temperature of which is measured. In some cases, various curtains can be used limiting the solar radiation effect. The problem of solar radiation disturbing automatic temperature measurements is still unsolved.

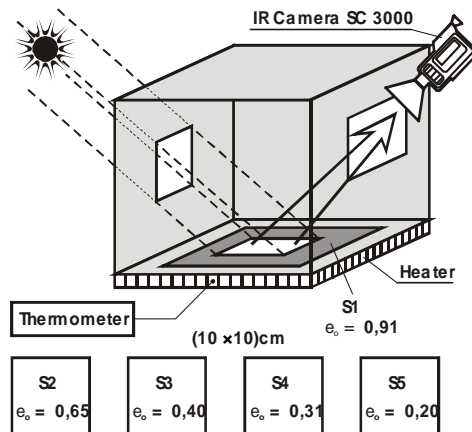


Fig. 1. Measuring set-up for investigations of sun radiation influence on object temperature measurements.

A measuring set-up has been built for investigations of sun radiation influence on the error of temperature measurement in field conditions (Fig. 1). The temperature of metal plates S1–S5 having various emissivities was measured. The plates were subsequently situated inside a housing to have them in the field of view of a thermovision camera. The distance between the camera’s objective and the plate was 120 cm.

Sun radiation reaches the examined plate through a rectangular hole cut in the front wall of the housing to illuminate only a part of the investigated plate. Due to this, simultaneous measurement of the temperature of the plate’s part reached by sun radiation (in Fig. 1 denoted with lighter colour) and the part not reached by sun radiation (darker colour) is made. Sun rays, after reflection from the investigated plate propagate along an optical axis of a thermovision camera (Fig. 2).

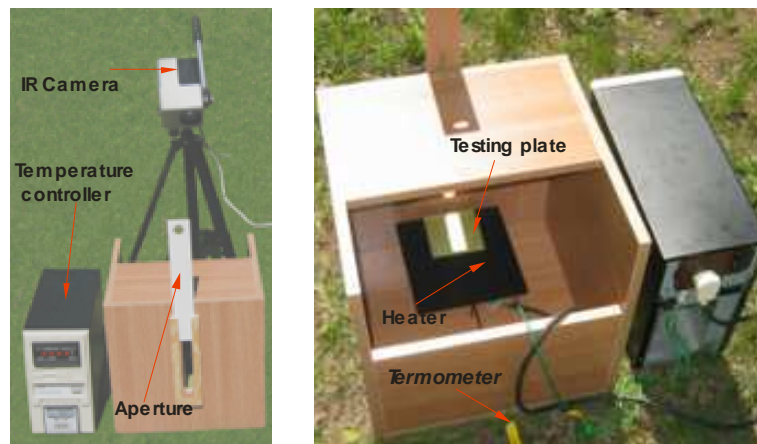


Fig. 2. The overall view of the test stand.

In order to eliminate the heating effect in the investigated plates caused by incident sun radiation, a rectangular hole was opened only for the measurement duration, *i.e.*, for about 2 s. The temperature of the investigated plates was stated with a heater and monitored with a thermometer.

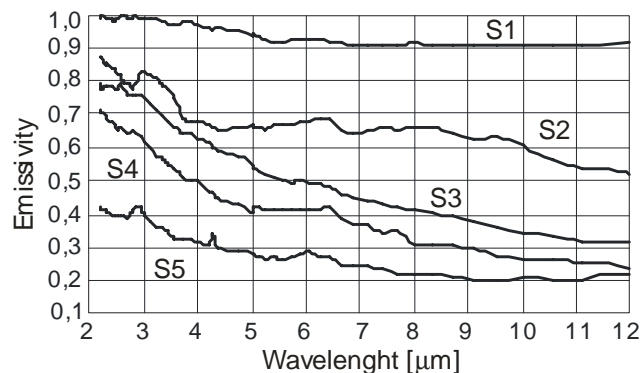


Fig. 3. Spectral emissivity of S1–S5 plates.

The spectral emissivity of the plates was determined using a Specord 71 IR spectrophotometer (Fig. 3). The emissivity averaged for a given range of camera operation was introduced into a thermovision camera. Fig. 4 shows a thermogram of a plane, painted aluminium plate illustrating the influence of the reflected solar radiation on the measurement result. The real temperature of the plate was 285 K. The rectangular area that can be seen in the figure was illuminated with sun light (intensity of $24 \mu\text{W}\cdot\text{cm}^{-2}$) only for the time of the thermogram performance.

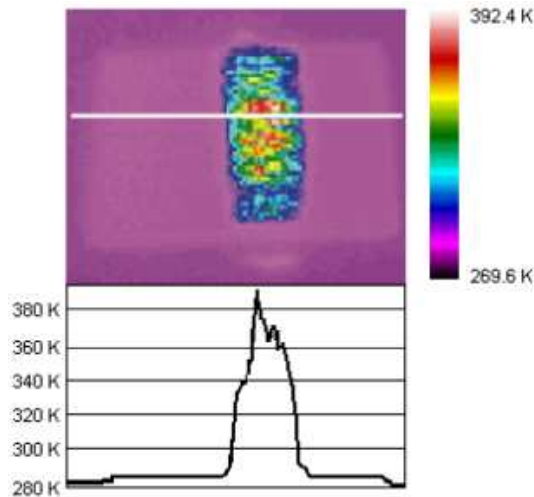


Fig. 4. Thermogram of a plate, with an emissivity $\varepsilon = 0.9$ and temperature $T = 285$ K, illuminated by solar radiation, made with a thermal imaging camera Therma CAM SC3000 working in the 8–9 μm infrared range. Below, the profile of temperature distribution along the straight line.

The values of temperature at the illuminated and non-illuminated areas of the same element can differ even from several to hundred degrees [1]. In such a case, the measurement should be repeated several times at various observation points. When an object’s surface is not plane, an effect of reflected sun radiation can be observed even after the change of a camera position with reference to an object. For IR pyrometers, in which the result is not presented as a thermogram but as a single value, interpretation of the result is much more difficult. The trials are undertaken to reduce the influence of solar radiation on remote temperature measurements [2].

At present, there are no available pyrometers having a correction system or a system for solar radiation elimination. Some special multispectral pyrometers are known which deliver the information about the measurement error caused by solar radiation [3] and the necessity of measurement repetition.

2. Model for determination of object temperature

2.1. Taken symbols

Energetic exitance of an absolute blackbody of temperature T , for a given spectral range $\lambda_1\text{--}\lambda_2$, results from the Planck $M(T)$ relation.

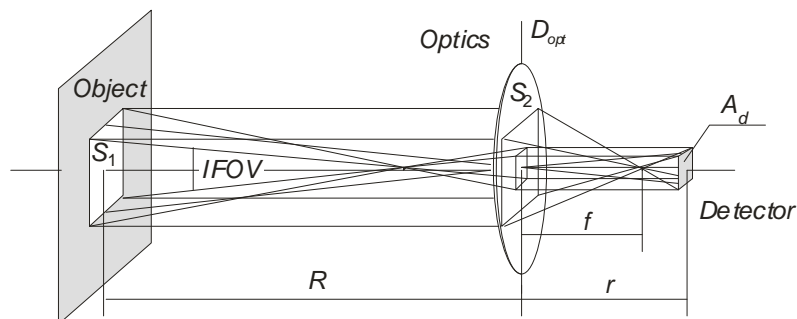


Fig. 5. Geometrical relations in an optical unit with the object focused on a detector (S_2 – working aperture of optics, S_1 – field of view, R – distance between object and optics, r – distance between optics and detector, D_{opt} – diameter of optics, f – optics focal length).

The power of radiation reaching the detector’s surface is (Fig. 5):

$$P(T) = qM(T), \quad (1)$$

where q is the construction constant resulting from the pyrometer design (Fig. 5):

$$q = \left(D_{opt} \operatorname{tg} \frac{IFOV}{2} \right)^2. \quad (2)$$

A design coefficient can be written in an equivalent form [4, 5]:

$$q = \frac{A_d}{4F^2 \left(1 + \frac{r}{R} \right)^2}, \quad (3)$$

where A_d is the detector area or a single pixel in a detector array and F – number (ratio of focal length to working aperture).

2.2. The Sun radiation

In real measuring conditions, the power of radiation reaching the input aperture of an optical system of a measuring device depends on many factors. The most important are radiant properties of the object itself which are determined by its temperature and emissivity. In measuring practice, most frequently the emissivity value is not known and even the use of tables does not ensure assumption of its proper value. It is because the emissivity depends on such factors as, e.g., structure and oxidation degree of a surface, its temperature, observation direction, and spectral range for which it will be determined or sometimes will be eliminated by some, specially designed, optical system for emissivity compensation [8, 9].

The Sun radiation temperature is approximately 5900 K. A spectral distribution of solar radiation is best approximated by the spectral distribution of an absolute blackbody with a temperature of 5770 K, the size of which corresponds to Sun's size [4]. This body emits the same radiation in all directions. Before it reaches the Earth, it is absorbed or scattered in the atmosphere. The ratio of solar radiation intensity, measured outside the Earth atmosphere $E_e(\lambda)$ to the intensity of solar radiation reaching the Earth surface $E_S(\lambda)$, determined for particular wavelengths is called the spectral permeability coefficient of the earth atmosphere $\tau_E(\lambda)$. A detailed determination of $\tau_E(\lambda)$ requires consideration of a lot of factors and parameters describing the atmosphere. The most important are: content and condensation degree of steam, temperature, atmospheric pressure, thickness of Earth's atmosphere and concentration of gas and aerosols contained in it.

The intensity of the total solar radiation E_S , in the chosen spectral range λ_1 – λ_2 , can be determined as:

$$E_S = \int_{\lambda_1}^{\lambda_2} \tau_E(\lambda) E_e(\lambda) d\lambda. \quad (4)$$

The spatial distribution of a solar radiation beam, after its reflection from the object's surface, depends on the type of radiation reflection [5, 6]. It can be a specular reflection (regular reflection), occurring for the reflection from a plane polished surface, diffuse reflection occurring for the reflection from a rough surface, directional diffuse reflection (mixed reflection, hybrid reflection) showing the features of both specular reflection and diffuse ones. Thus, spatial distribution of solar reflection reaching a detector depends on a surface's structure and its roughness [7]. The cases of specular reflection and diffuse reflection are extreme ones and rarely occur in reality. The solar radiant exitance P_S for directional diffuse reflection can be expressed as:

$$P_s = \begin{cases} A_d \left(\frac{R-f}{f} \right)^2 E_s = \left(2R \operatorname{tg} \frac{IFOV}{2} \right)^2 E_s, & \alpha = \beta \\ q E_s, & \alpha \neq \beta \end{cases} \quad (5)$$

where α is an angle incidence of solar radiation and β is an angle reflection of solar radiation.

Among other factors affecting the power of radiation reaching the input aperture of an optical system of a measuring device, the following factors should be mentioned: the radiation reflected from an object's surface, absorption, as well as dissipative and radiant properties of the atmosphere. The total power of radiation reaching the input aperture of an optical system can be expressed for typical measuring conditions as [6]:

$$P_c = \varepsilon \cdot \tau_a \cdot P(T) + (1 - \tau_a) \cdot P_a(T_a) + (1 - \varepsilon) \cdot \tau_a \cdot P_{ot}(T_{ot}), \quad (6)$$

where ε is the object's emissivity, τ_a is the atmosphere transmission coefficient between the object and the optical system, $P(T)$ is the radiant exitance of a blackbody of the temperature T , exitance $P_a(T_a)$ is the radiant exitance of atmosphere of temperature T_a , and $P_{ot}(T_{ot})$ is the radiant of the ambient of temperature T_{ot} . If we assume that each of the components of the radiant exitance, *i.e.*, $P(T)$, $P_a(T_a)$, and $P_{ot}(T_{ot})$, generates at the detector output, a signal voltage proportional to this power, $U(T)$, $U_a(T_a)$, $U_{ot}(T_{ot})$, respectively, the expression for the total value of a voltage signal is as follows:

$$U_c = \varepsilon \cdot \tau_a \cdot U(T) + (1 - \tau_a) \cdot U_a(T_a) + (1 - \varepsilon) \cdot \tau_a \cdot U_{ot}(T_{ot}). \quad (7)$$

In devices in which the above relation is used for the determination of the object's temperature, the user should estimate and introduce the corrections for such parameters as: the object emissivity ε' , the coefficient of atmosphere transmission τ_a' , the atmosphere temperature T_a' , and the ambient temperature T_{ot}' . By solving Eq. (6), with respect to $U(T)$, and considering the introduced corrections we have:

$$U(T_o) = \frac{1}{\varepsilon' \tau_a'} U_c - \frac{1 - \tau_a'}{\varepsilon' \tau_a'} U_a(T_a') - \frac{1 - \varepsilon'}{\varepsilon'} U_{ot}(T_{ot}'). \quad (8)$$

Knowing the value of the voltage $U(T_o)$, the object's temperature T_o can be determined on the basis of a calibration characteristic of the device. The subscript *o* is introduced to distinguish a calculated value from a real one. The relative error of the object temperature determination:

$$\delta_T = \frac{T' - T_o}{T_o} 100\%, \quad (9)$$

depends mainly on the difference between the real values of the parameters of Eq. (7) and the introduced ones. It should be noticed that using this method, the assumption was taken that particular components of radiation are described by Lambert's law, what in the case of specular reflection and directional diffuse reflection is not fulfilled.

2.3. Calculation results

It was taken for the above presented mathematical description of phenomena that for short distances $\tau_a=1$. Exemplary calculations were carried out for a solar radiation spectrum determined with the PcModWin 3.0 program for a summer atmosphere, country conditions, visibility of 23 km, and a deviation angle of the Sun from the zenith $\theta_z=30^\circ$. Total intensity of solar radiation (E_s) was calculated for typical operation ranges of long-wavelength IR pyrometers and thermal cameras, *i.e.*, 8–9 μm , 8–12 μm , and 7.5–13 μm (Fig. 6).

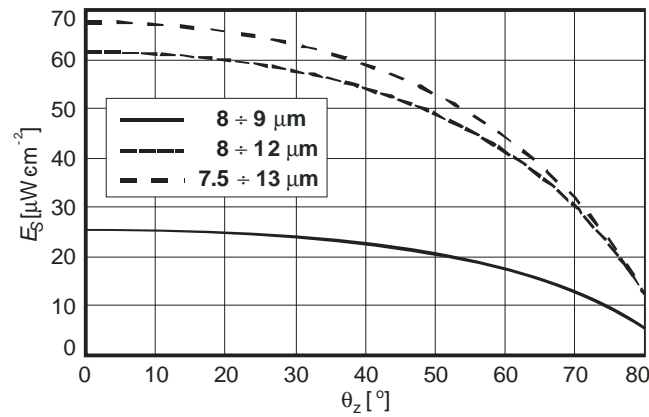


Fig. 6. Total solar irradiance vs. zenith solar angle for selected infrared ranges.

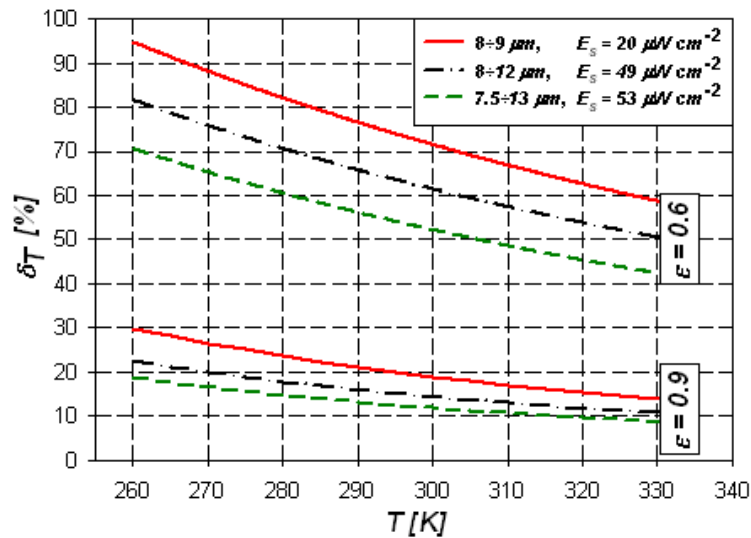


Fig. 7. Calculated relative error of temperature reading for an object with emissivity: $\varepsilon = 0.6$ and $\varepsilon = 0.9$; for three infrared ranges. Summer model atmosphere and rural profile of aerosol; $V_{is} = 23$ km; $\theta_z = 50^\circ$.

For calculations of the relative error of a temperature reading, the following values of input parameters were assumed: $R=120$ cm, $f=3.5$ cm, $D_{opt}=5$ cm, $IFOV=1.1$ mrad, and $T=243\text{--}363$ K. The values of the relative temperature error of objects with emissivity $\varepsilon=0.9$ and $\varepsilon=0.6$ are presented in Fig. 7.

It results from the obtained results that the relative error of temperature measurement is caused by solar radiation and depends both on the object's emissivity and its temperature. Also, it depends on the width of the detection band. In general, a narrower bandwidth for a constant initial wavelength gives a larger error than broadband. It results from the fact that the power of object radiation decreases in relation to the power of solar radiation reflected from it. Moreover, the error increases with increasing intensity of solar radiation.

3. Measurement method

The method of temperature measurement of an object under solar radiation consists in simultaneous measurements of a radiant exitance in the short-wavelength band $2.4\text{--}3.4$ μm and in the long-wavelength band. The observation area of an optical system is identical for both bands (Fig. 8). The short-wavelength band is significantly far from the long-wavelength band. Thus, no signal changes at the detector output, caused by object radiation in this band are observed. The actual temperature measurement is made in the long-wavelength band but

the short-wavelength band is used only for detection of solar radiation reflected from an object.

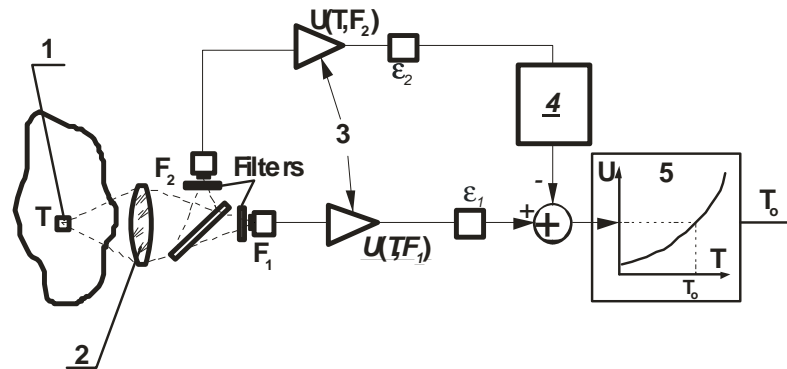


Fig. 8. Scheme of a pyrometer with the unit for solar radiation compensation: 1) measurement field; 2) optics; 3) signal processing; 4) correction set of solar radiation; 5) signal analysis set.

When an object is illuminated with solar radiation, the signal value increases at the outputs of both detectors. Knowing the signal value at the output of a short-wavelength detector, the signal value at the output of the long-wavelength detector should be corrected, the same the error of temperature readout caused by adding the reflected solar radiation should be reduced or totally eliminated. The correction is made by substituting the value of the signal measured in the short-wavelength band into the correction function and thus, the obtained signal value is subtracted from the signal measured at the long-wavelength detector output. It should be mentioned that the object's emissivity in the short-wavelength band can be different than in the long-wavelength band. The device user has to know the emissivity values.

Basing on calculations with the PcModWin 3.0 program and using the characteristics of solar radiation intensity obtained with the SR-5000 spectroradiometer, it can be shown that the changes of solar radiation in 2.4–3.4 μm band are best correlated with the changes of solar radiation in the long-wavelength range (LWIR). A decrease/increase in solar radiation intensity in the 2.4–3.4 μm range is accompanied by a decrease/increase in the value of solar radiation intensity in the long-wavelength range. Thus, it is possible to determine the solar radiation intensity in the LWIR band as a function of solar radiation intensity in the 2.4–3.4 μm range for any type of earth atmosphere.

To verify the above statement:

- 180 spectral distributions of solar radiation in the LWIR range were analyzed. These distributions were obtained with the PcModWin program for the following models of atmosphere: Tropical, MidLatitude Summer, MidLatitudeWinter, 1976 US Standard, for various aerosol models Rural VIS=23 km, Rural VIS=5 km, Navy Maritime, Maritime VIS=23 km, Urban VIS=5 km, and sun deviation angles from the Zenith from 0° to 80° with a step of 10°;
- total intensity of solar radiation in the correction band 2.4–3.4 μm and in selected long-wavelength detection ranges 8–9 μm , 8–12 μm , and 7.5–13 μm was determined;
- the obtained data were approximated with a third-degree polynomial of the form:

$$E_{S,LW} = a_1 (E_{S,SW})^3 + a_2 (E_{S,SW})^2 + a_3 E_{S,SW} + a_4, \quad (10)$$

where $E_{S,SW}$ is the intensity of solar radiation in the short-wavelength correction band of 2.4–3.4 μm , $E_{S,LW}$ is the intensity of solar radiation in the selected detection ranges 8–9 μm , 8–12 μm , or 7.5–13 μm , a_1 – a_4 are the polynomial coefficients determined for particular LWIR ranges. The changes of solar radiation intensity in the ranges 8–9 μm and 8–12 μm , obtained

from the calculations as a function of solar radiation intensity in the band 2.4–3.4 μm are shown in Fig. 9 and for the band 7.5–13 μm in Fig. 10.

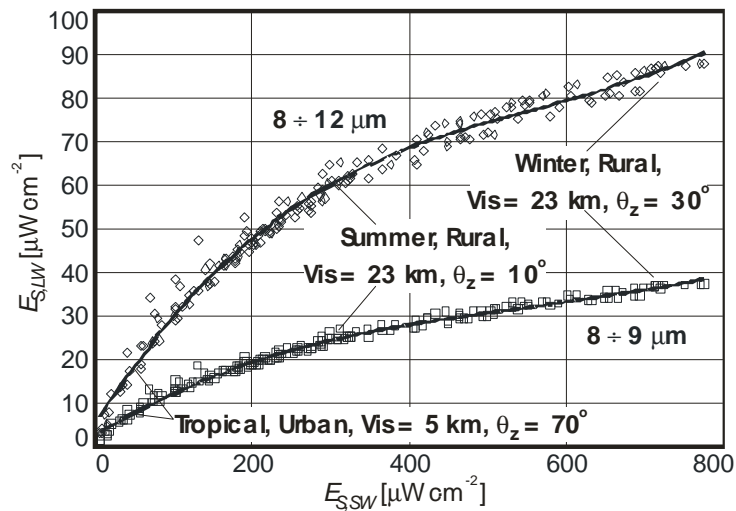


Fig. 9. Solar irradiance in 8–9 μm and 8–12 μm ranges vs. solar irradiance in the 2.4–3.4 μm band.

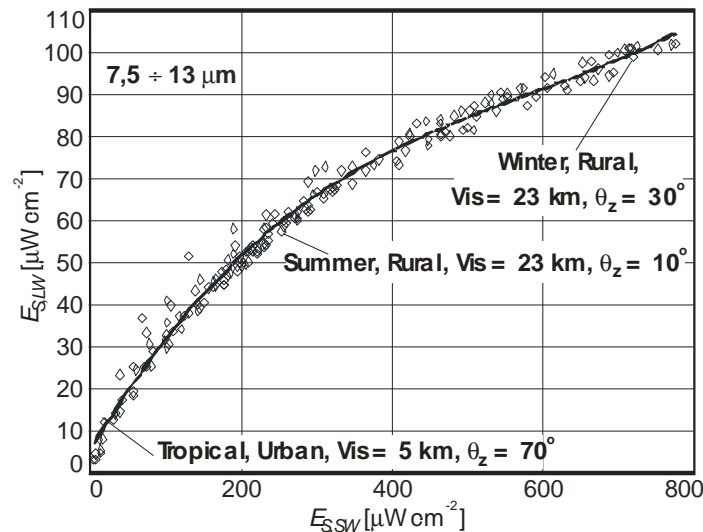


Fig. 10. Solar irradiance in 7.5–13 μm range vs. solar irradiance in the 2.4–3.4 μm band.

The efficiency of this method can be estimated by considering the decrease in the relative error of temperature measurement when the value of solar radiation is compensated according to Eq. (10). To do it, the difference ΔE_S between the approximating curve and the real values of solar radiation should be determined, i.e. the value of non-compensated solar radiation in the process of temperature measurement is equal to:

$$\Delta E_S = E_{S,LWIR} - E_{S,LW}. \quad (11)$$

When $\Delta E_S = 0 \mu\text{W cm}^{-2}$, the measurement of an object temperature will be error-free (accurate) because the value of the compensated intensity of the solar radiation $E_{S,LW}$ is the same as its real value $E_{S,LWIR}$.

For $\Delta E_S > 0 \mu\text{W cm}^{-2}$, the indicated object's temperature will be higher than the object temperature because only a part of solar radiation will be compensated. For $\Delta E_S < 0 \mu\text{W cm}^{-2}$, the indicated object's temperature will be lower than the object temperature because the compensated value of solar radiation intensity is higher than the real one. It was taken for

calculations that $\Delta E = \pm \Delta \bar{E}_S$, where $\Delta \bar{E}_S$ is the average value of the intensity of non-compensated solar radiation:

$$\Delta \bar{E}_S = \pm \frac{1}{180} \sum_{i=1}^{180} |E_{S,LWIR}^i - E_{S,LW}^i| \quad (12)$$

The value $\Delta \bar{E}_S$ for the detection bands 8–9 μm , 8–12 μm , and 7.5–13 μm is 0.7 $\mu\text{W cm}^{-2}$, 1.9 $\mu\text{W cm}^{-2}$, and 2.2 $\mu\text{W cm}^{-2}$, respectively. The calculation results of the maximal error of temperature measurement using a pyrometric method with compensation of solar radiation are given in Figs 11–13.

The obtained calculation results confirm the correctness of the chosen correction band and the proposed method of temperature measurement. The smallest errors of temperature measurements of objects illuminated with solar radiation are obtained for the correction band 2.4–3.4 μm and the measuring band 7.5–13 μm . The obtained calculation results show that for the objects with an emissivity $\varepsilon \geq 0.6$, i.e., for the majority of industrial objects (e.g. zinc coated sheets or steel sheets), the measured temperature does not differ from the real value more than 10%.

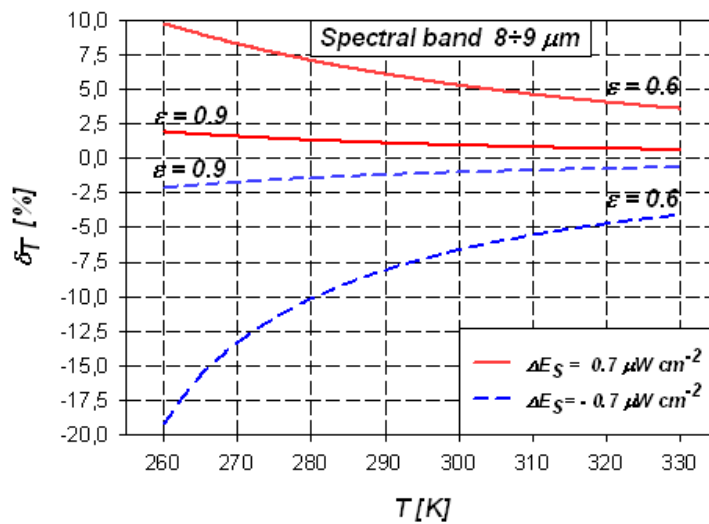


Fig. 11. Relative error of temperature readout of an object with an emissivity $\varepsilon = 0.6$ and $\varepsilon = 0.9$ for the measurement band 8–9 μm and $\Delta E_S = \pm 0.7 \mu\text{W cm}^{-2}$.

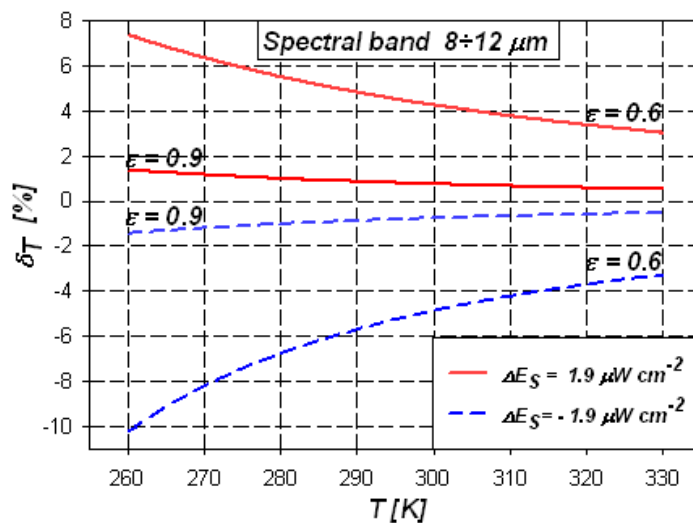


Fig. 12. Relative error of temperature readout of an object with an emissivity $\varepsilon = 0.6$ and $\varepsilon = 0.9$ for the measurement band 8–12 μm and $\Delta E_S = \pm 1.9 \mu\text{W cm}^{-2}$.

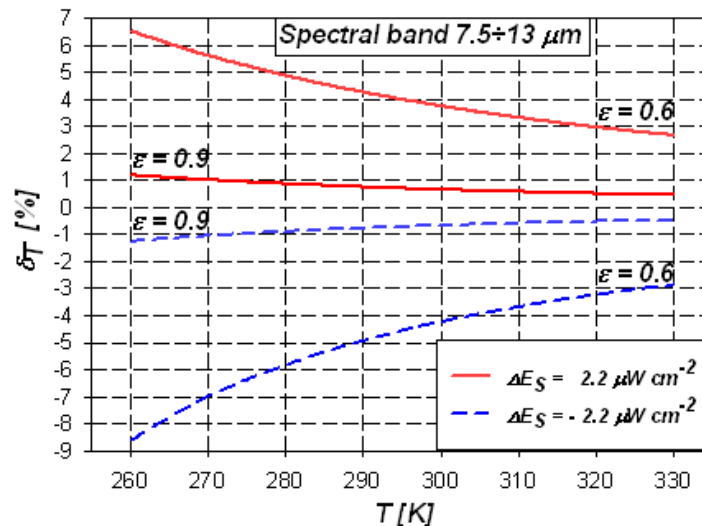


Fig. 13. Relative error of temperature readout of an object with an emissivity $\varepsilon = 0.6$ and $\varepsilon = 0.9$ for the measurement band 7.5–13 μm and $\Delta E_S = \pm 2.2 \mu\text{W cm}^{-2}$.

4. Conclusions

A new method of compensation of solar radiation influence on measurement results obtained with pyrometers of thermal cameras operating in the IR long-wavelength range was presented. Computer simulation of this method allows to predict that its application in an algorithm of temperature determination in pyrometers and thermal cameras will reduce measurement errors, in some cases even of one order of magnitude. Basing on the simulations presented in the article, it is planned to make a pyrometer model in which the effect of solar radiation influencing the results of remote temperature measurements will be reduced.

References

- [1] Madura, H., Kołodziejczyk, M., (2005). Influence of sun radiation on results of non-contact temperature measurements in far infrared range. *Opto-Electronics Review*, 13, 253–257.
- [2] Bielecki, Z., Chrzanowski, K., Matyszek, R., Piątkowski, T., Szulim, M. (1999). Infrared pyrometer for temperature measurement of objects of both wavelength- and time-dependent emissivity. *Optica Applicata*, 29, 284–292.
- [3] H. Madura, T. Piątkowski, E. Powiada: “Multispectral precise pyrometer for measurement of seawater surface temperature”. *Infrared Physics and Technology*, no. 46, 2004, pp. 69–73.
- [4] Riedl, M.J., (2001). *Optical Design, Fundamentals for Infrared Systems*. Bellingham, Washington: SPIE Press.
- [5] Holst, G.C. (1998). *Testing and Evaluation of Infrared Imaging Systems*. Bellingham, Washington: SPIE Press.
- [6] Zissis, J.G. (1993). The Infrared&Electro-Optical Systems Handbook. *Sources of Radiation*, 1, Bellingham: SPIE Press.
- [7] Nayar, S.K., Ikeuchi, K., Kanade, T. (1989). Determining shape and reflectance of lambertian, specular, and hybrid surfaces using extended sources. *International Workshop on Industrial Application of Machine Intelligence and Vision*. Tokyo.
- [8] Madura, H., Kastek, M., Piątkowski, T. (2007). Automatic compensation of emissivity in three-wavelength pyrometers. *Infrared Physics and Technology*, 51, 1–8.
- [9] Madura, H., Piątkowski, T. (2004). Emissivity compensation algorithms in double-band pyrometry. *Infrared Physics and Technology*, 46, 185–189.